Pol. J. Environ. Stud. Vol. 32, No. 2 (2023), 1313-1322
DOI: *10.15244/pjoes/155874* ONLINE PUBLICATION DATE: 2022-12-23

Original Research

Evaluation of the Effect of Bimetallic Organic Framework M/Fe-MOF (M=Ni, Co) on the Removal of Congo Red Dye

Thi Cam Quyen Ngo[1,2,*], Thi Nhu Dung Nguyen[3], Hung Dung Chau[1,2], Bich Ngoc Hoang[1,2]

[1]Institute of Applied Technology and Sustainable Development, Nguyen Tat Thanh University, Ho Chi Minh City, Vietnam
[2]Full Affiliation, Address Faculty of Environmental and Food Engineering, Nguyen Tat Thanh University, Ho Chi Minh City, Vietnam
[3]Ho Chi Minh University of Natural Resource and Environment, Ho Chi Minh City, Vietnam

Received: 9 September 2022
Accepted: 18 October 2022

Abstract

In this study, we investigated the adsorption process of organic Congo red (CR) by M/Fe-MOF (M=Co, Ni) materials. The results of the study show that the optimal adsorption capacity of the materials under the optimal conditions is as follows: Adsorbent weight 0.1 g/L and pH8 for all 3 materials. At the concentration of colorant CR 75 mg/L, the adsorption capacity reached 530 mg/g for Co/Fe- MOF materials; for Ni/Fe-MOF materials, the adsorption capacity reached 560 mg/g, at the colorant concentration CR 140 mg/L; for Fe-MOF materials, the adsorption capacity reached 523 mg/g, at the colorant concentration CR 120 mg/L. The experimental data are consistent with Langmuir and PSO models for both M/Fe-MOF materials (M=Co, Ni). Research results on the reuse process of M/Fe-MOF (M=Co, Ni) materials show that the material is reused 4 times. With this result, it can be considered as the first step to improve the efficiency of pigment adsorption in the current water pollution treatment problem.

Keywords: metal-organic framework, adsorption, Congo red, thermodynamics and equilibrium isotherms

Introduction

Water is an extremely important resource for human sustainable development. Currently, along with the development of industrialization and modernization, environmental pollution in general and water environment is a burning problem for us. Textile dyeing companies as well as other chemical companies consume large quantities of dyes, resulting in highly soluble dyes that become a major source of water pollution. Organic dyes are not easily decomposed, the discharge of untreated wastewater containing many dyes into the aquatic environment causes serious consequences for the ecosystem as well as human

*e-mail: ntcquyen@ntt.edu.vn

health (allergic reactions). skin, mutagenic, teratogenic, and carcinogenic) [1].

To date, many methods, including photodegradation, adsorption, coagulation, and membrane filtration, have been studied to remove industrial pollutants. Among the mentioned methods, adsorption is the most favored for dye removal due to many advantages such as fast operation, high efficiency, and ease of handling. Traditional adsorbents, such as activated carbon, zeolites, silica microspheres and natural fibers, have been used to remove pollutants; however, their applications are limited due to inadequate adsorption capacity, relatively low thermochemical stability, and poor reusability [65]. To optimize the adsorption capacity and handle the dye contamination problem, research has been carried out on metal-organic framework materials. The metal-organic framework (MOF) is a new type of porous crystalline material composed of metal ions and organic ligands. Due to its special features, including high porosity, high specific surface area and catalytic efficiency, as well as magnetic and electrochemical capabilities, MOF has many applications, namely adsorption applications. MOF has attracted a lot of interest in the field of organic dye removal, for example, Zn-MOF [2] , Al-MOF [3], Fe-MOF [4] and Cu-MOF [5].

Some researchers have focused on using MOFs to remove environmental pollutants such as organic dyes from wastewater [6-9]. In 2020, Author Gulzhian I. Dzhardimalieva et al studied several synthetic pathways for metal-organic frameworks (MOFs) to remove organic dyes methylene blue (MB), Congo red (CR) and methyl violet (MV). Dye adsorption follows pseudo-first order kinetics [10]. In 2021, author Giulia Rossella Delpiano et al studied the adsorption of Malachite Green and Alizarin Red S dyes using Fe-BTC metal-organic framework as adsorbent. In this study, the iron-based Fe-BTC MOF material, prepared by a rapid, aqueous, aqueous process, was used as an adsorbent to remove alizarin red S (ARS) and malachite blue dyes. (MG) from the water. Experimental results show that: optimal adsorption pH is 4, and at 298 K, adsorption equilibrium is reached in less than 30 minutes after pseudo-second-order kinetics [11]. Most recently (in 2022), author Ngan Tran Thi Kim research Co-doped Fe-MOF bimetallic organic framework materials at different ratios were synthesized based on the solvothermal method. The post-synthesized materials were evaluated for their ability to absorb various dyes, including Methylene Blue (MB), Methyl orange (MO), Congo red (CR), and Rhodamine (RhB). The highest adsorption capacity of MB dye by 0.3 CoFe-MOF reaches up to 562.1 mg/g at pH 10, the initial concentration of MB of 200 mg/L, after 90 min. The adsorption efficiency on the mixed system of cationic (MB) and anionic (MO) dyes yielded the highest removal efficiency of 70% and 81%, respectively, after 30 min [12]. The author Zhen-Zhen Xue, research construction of Cu(I)-organic frameworks with effective sorption behavior for iodine and Congo red. The Cu(I)-organic network displays an excellent adsorption behavior toward iodine and efficient uptake and separation capacity for Congo red, which could be further deemed as a promising candidate for the treatment of wastewater [13].

This study evaluates the applicability of M/Fe-MOF bimetallic organic framework material (M=Co, Ni) in removing toxic dye Congo red from industrial waste. The adsorption characteristics and dye removal efficiency of Fe/M-MOF were investigated by influencing factors such as pH, time, initial concentration of dye and amount of adsorbent. To study the adsorption isotherm model, this thesis uses Langmuir, Freundlich, Temkin and Dubinin-Radushkevich models. For the adsorption kinetics, pseudo-first order (PFO), pseudo-second order (PSO), intraparticle diffusion and Elovich models were included. The reusability of the adsorbent was also evaluated by synthetic studies. In summary, through this study, MOF materials have shown useful properties in removing CR from water.

Material and Methods

This study investigates the influence of factors affecting the adsorption process: concentration, time, solution pH and mass on the adsorption efficiency of organic pigments (methyl blue). Weigh 0.001 g of material into 10 mL of organic colorant solution at different concentrations from 10 to 100 mg/L. Stir at a constant temperature of 200 rpm. Sampling over time, centrifuged to remove solids from solution using a Centrifuge PLC series centrifuge (5000 rpm, 10 min). Measure residual organic pigment concentration by UV-Vis. The expected product will be an organic pigment adsorption process with high efficiency. The tasks to be performed include time survey (for 5-480 minutes), organic colorant concentration survey (10-100 mg/L), solution pH survey (2, 4, 6, 8, 10), survey the material weight (0.05; 0.1; 0.2; 0.3 g/L).

The adsorption capacity was calculated according to the following formula:

$$q_e = \frac{C_0 - C_f}{W}.V = \frac{C_0 - C_f}{dosC}$$

In which qe (mg/g) represents the adsorption capacity, Co and Cf (mg/L) represent the color concentrations before and after adsorption, respectively. Dos C (g/L) represent the content of adsorbent and W (g) represent the mass of the adsorbent.

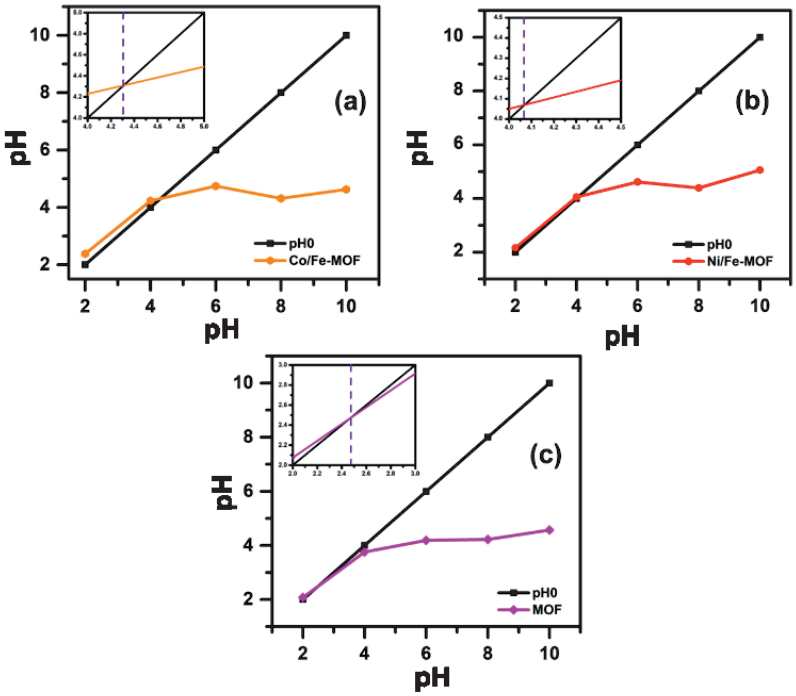

Fig. 1. Isoelectric curves of the materials a) Co/Fe-MOF, b) Ni/Fe-MOF, c) Fe-MOF.

Results and Discussion

Assessment of the Material's Advertisement Capability

Effect of pH Value on CR Adsorption Capacity

The pHpzc parameter of the material describes the state that the charge density on the surface when the pH variation reaches a value of zero [14]. Fig. 1. shows the pHpzc values of the materials in the order: 2.45 (MOF)<4.06(Ni/Fe-MOF)<4.3 (Co /Fe-MOF). Note that when the pH of the solution is lower than the pHpzc value, the surface of the material is positively charged, resulting in electrostatic forces between the anions and the positively charged functional groups on the surface. In contrast, when the surface is negatively charged at pH>pHpzc, there is a tendency to attract positively charged cations from the solution.

Fig. 2 shows the influence of pH value on the CR color adsorption capacity. Congo Red is an example of a diazo dye, and the initial pH affects the molecular form of CR in solution. When the pH decreases, the color of the CR solution changes from red to dark green, at pH 10-12 the solution has a different red color than the original red. The color changes with pH indicate that the degree and nature of the ionic character of the CR molecule are dependent on the pH of the medium [15]. The pH of the solution can significantly affect the CR adsorption efficiency of the adsorbent, related to the electrostatic interaction between the CR molecules and the adsorbent. Looking at the graph, we can see that the adsorption capacity of all 4 materials reached high values at pH 8 as follows: Co/Fe-MOF (81 mg/g), Ni/Fe-MOF (66 mg/g), respectively, MOF (38 mg/g). At pH above 8, reduction of adsorption occurs due to repulsion between the anionic dye molecules and the negatively charged adsorbent surface. We chose pH 8 as the best pH value to conduct the next experiments.

In general, the surface groups on the adsorbent are less protonated at higher pH, so the surface of the metal-based adsorbent is less positively charged, leading to a weaker electrostatic attraction with the S^+ anion groups. in the CR molecule. In most cases, the CR adsorption capacity decreased with increasing pH of the CR solution. For example, the CR adsorption capacity of $NiO–SiO_2$ hollow microspheres decreased continuously

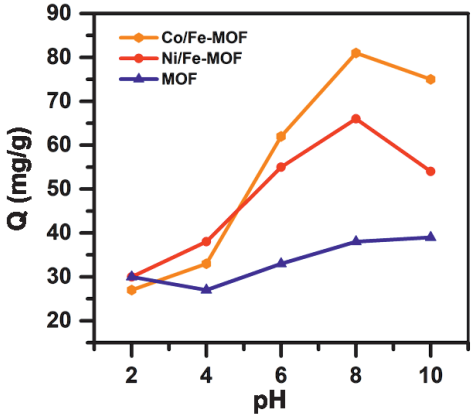

Fig. 2. Effect of pH value on the adsorption capacity of M/Fe-MOF materials (M=Co, Ni).

with increasing pH from 4–12 [16]. However, Bao et al. (2019) [17] explored the CR adsorption capacity of porous $NiCo_2O_4$ nanosheets with the change of pH and found that the largest amount of CR adsorption occurred at pH = 6, while the zeta potential decreased with pH increased from 4 to 12. The porous $NiCo_2O_4$ nanosheets exhibit a decrease in adsorption capacity when the pH is decreased from 6 to 4, which is attributed to the partial resolution of the $NiCo_2O_4$ nanosheets under acidic conditions. Therefore, we choose pH8 as a condition for the following experiments.

Effect of Time on CR Adsorption

Fig. 3 shows that the materials reach the adsorption equilibrium time respectively as follows: at the time point of 60 minutes, the materials Ni/Fe-MOFs (205 mg/g), Co/Fe-MOF (285 mg/g) and Fe-MOF (185 mg/g) reached the highest value of adsorption capacity. After this time, the adsorption capacity reached equilibrium, the adsorption capacity decreased insignificantly. The solution will be shaken continuously in this experiment so that the external mass transfer coefficient increases leading to faster adsorption of the dye molecules. Through this experiment, we found that the modified material has a higher adsorption capacity and faster equilibrium time than the original material (Ni/Fe-MOFs, Co/Fe-MOF).

In an experiment to investigate the time of the MOF Fe_3O_4@MIL-53(Al) material adsorbing CR, the adsorption time was investigated from 20 to 300 minutes. At 0-180 min, the adsorption capacity of CR increased rapidly. From 180 to 300 min, the adsorption capacity of CR did not increase significantly with increasing time, so 180 min is the adsorption equilibrium time of CR [18].

Therefore, we choose a time of 60 minutes for the next adsorption experiments for Ni/Fe-MOFs, Co/Fe-MOF, Fe-MOF materials. As for the Mn/Fe-MOF materials, the 90-minute hook was chosen to conduct the next experiments.

Effect of Adsorbent on CR Adsorption Capacity

First, the amount of adsorbent has a great influence on the applicability of the material, so optimizing the amount of adsorbent will help reduce the actual cost. Here, the amount of substance to be investigated ranges from 0.05 to 0.2 g/L. To investigate the effect of material content on the adsorption capacity of CR organic pigments, we fixed other conditions of the experiment.

As observed from Fig. 4, the CR color adsorption capacity reached its maximum at 0.1 g/L dose and then gradually decreased. For example, a Co/Fe-MOF material of nearly 152 mg of CR pigment is absorbed per gram of material at an amount of 01 g/L, while that value for a dosage of 0.2 g/L is only about 63, 5 mg. The reason for this phenomenon is related to the effective sites on the material. Only when the effective site of the material is fully utilized can maximum efficiency be achieved [19]. When the amount of adsorbent is large, too many adsorbent particles in the solution will lead to overlapping of the adsorption binding sites, reducing the equilibrium adsorption capacity of CR [20].

The increase in CR color removal with increasing amount of material is due to an increase in the number of adsorption sites of the material in the aqueous solution. However, CR color removal is not beneficial when high material dosages are used, possibly because the significant addition of material particles can alter the physical properties of the solid/liquid (ie. viscosity), which limits the diffusion of solute molecules to the surface of the material. Therefore, to minimize the amount of material used, we carry out experiments with an optimal dose of 0.1 g/L to reduce CR pollution in water.

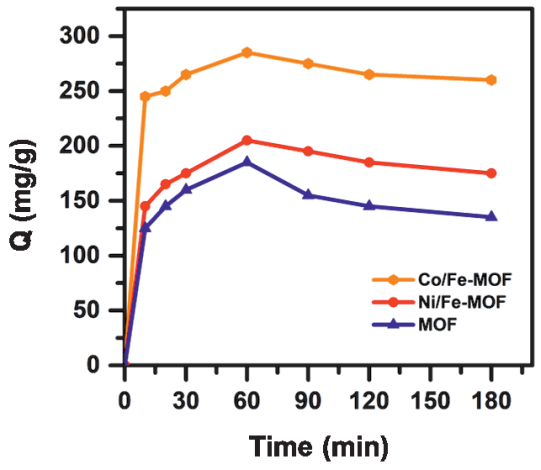

Fig. 3. Effect of time on the adsorption capacity of M/Fe-MOF materials (M=Co, Ni).

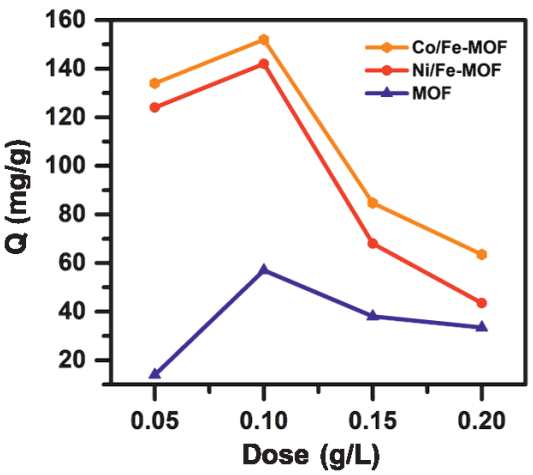

Fig. 4. Effect of amount of adsorbent on the adsorption capacity of M/Fe-MOF materials (M=Co, Ni).

In a previous study on Fe-MIL-88NH_2 material, the CR removal rate was first increased when the dose of Fe-MIL-88NH_2 was increased from 5 mg to 15 mg. As the amount of adsorbent increased, the surface area and adsorption site of the adsorbent increased, which improved the CR removal rate. When the Fe-MIL-88NH_2 dose is above 15 mg, the CR removal rate can reach 87.2%, and the elimination rate is little changed with further increase in the Fe-MIL-88NH_2 dose [20].

Effect of Initial Concentration of CR Colorant on Adsorption Capacity

The effect of concentration on the adsorption of organic pigments on materials was investigated from 5 mg/L to 160 mg/L, respectively, for CR pigments.

The results in Fig. 5 show that the adsorption capacity increases with increasing initial antibiotic concentration. The adsorption rate increased almost linearly, and the CR adsorption capacity peaked at approximately 75 mg/L for Co/Fe-MOF, 120 mg/L for Mn/Fe-MOF and MOF, and 140 mg/L for Mn/Fe-MOF and MOF. with Ni/Fe-MOF. The increase in initial concentration increases the interaction between CR molecules and the adsorbent, the adsorption process will take place more strongly. Therefore, this topic has selected this concentration range to study the adsorption isotherm for further experiments.

In a previous study, four different concentrations, 50, 100, 150 and 200 mg/L, respectively, were chosen to investigate the effect of the initial dye concentration (C0) on the adsorption of CR onto Cabentonite. Results were obtained at 20ºC and pH 6.92 of the CR solution, with increasing the initial dye concentration from 50 to 200 mg/L, the amount of dye adsorbed by Ca-bentonite increased from 23.25 to 85.29 mg/g. The graph also shows that the adsorption of CR is fast at the beginning, and then becomes slower near the equilibrium. To explain this phenomenon, in the first stage, the adsorption process is fast due to the large number of vacancies on the surface, and after a while, the remaining surface vacancies will be difficult to adsorb. due to the repulsive force between the CR molecules adsorbed on the Ca-bentonite surface and the CR molecules in the solution phase. The adsorption process is highly dependent on the initial concentration of the solution [21].

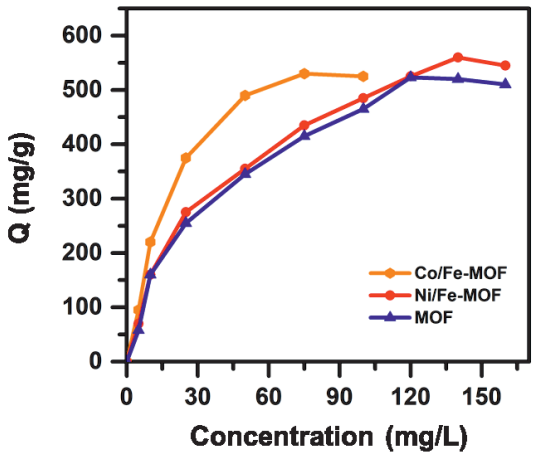

Fig. 5. Effect of initial concentration of CR colorant on the adsorption capacity of M/Fe-MOF materials (M=Co, Ni).

Surveying Models of Thermal and Dynamics of Advertisement

Isothermal Adsorption

Adsorption models were used to explain the mechanism, chemical affinity, and surface properties of CR adsorption. To evaluate the adsorption isotherm models of CR pigments on experimental data converted into various forms based on adsorption isotherm models: Langmuir, Freundlich, Temkin, D-R.

It can be seen in Fig. 6 that the four models have good compatibility with the experimental data and the calculated correlation coefficients R^2 are all greater than 0.8 as described in Table 1. However, based on the R^2 value, we see the correlation of the models appearing in the order: D-R < Freundlich < Temkin < Langmuir. Therefore, adsorption occurs on a heterogeneous surface, there is an interaction between the adsorbent and the adsorbent, the adsorption center has heat of adsorption occurring, and the heat of adsorption of all molecules decreases linearly count.

Based on the calculated data and the correlation coefficient of each model, the Langmuir isotherm model shows the highest correlation coefficient (R^2 = 0.9895 - 0.99309), showing high compatibility of the Langmuir isotherm model for the investigated data. Therefore, the adsorption of CR onto M/Fe-MOF is a monolayer and homogeneous surface adsorption. In other words, the adsorbed substances form a monomolecular layer, and adsorption can only occur at a finite (fixed) number of equally defined sites. In addition, there are no lateral interactions between the adsorbed molecules, even on neighboring sites [22].

In the study on the MB and MG color adsorption of Fe_3O_4@AMCA-MIL53(Al) materials, Alqadami A. A. et al. investigated and concluded about the correlation between the Langmuir isotherm model for the materials. data on the adsorption of both colors on the material surface [23]. Another study in 2020 on the adsorption of anionic dyes on Sn(II)-BDC MOF materials, the Langmuir isotherm model was proved again for its high compatibility with the adsorption process [24]. Also in 2020, Valadi F. M. and colleagues also concluded that the Langmuir isotherm model with compatibility R^2 = 0.9986 is suitable for the CR color adsorption process on La-MOF-NH_2@Fe_3O_4 materials. than the Freundlich model (R^2 = 0.7879) [25].

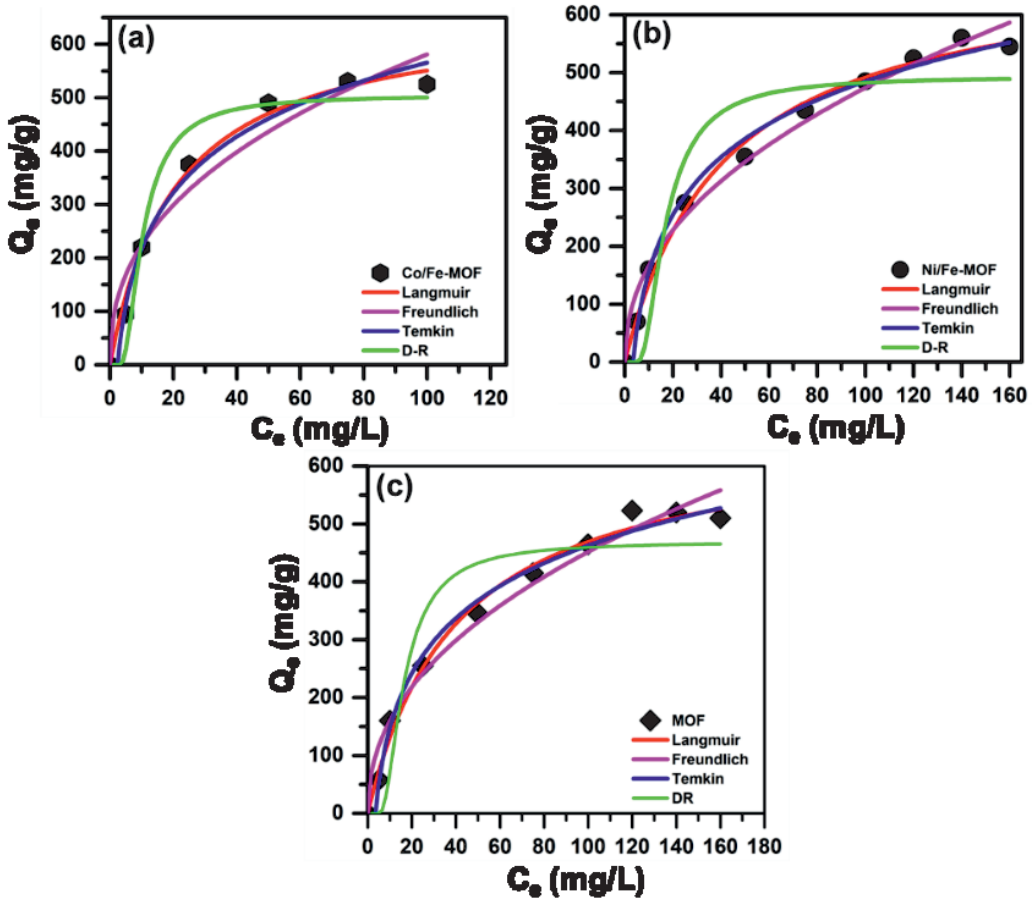

Fig. 6. The adsorption isotherm model of the materials a) Co/Fe-MOF, b) Ni/Fe-MOF, c) Fe-MOF.

Adsorption KInetics

The adsorption kinetics of M/Fe-MOF materials (M=Co, Ni) were studied using four models including PFO, PSO, Elovich and Bangham. As seen in Fig. 7 the adsorption capacity increased rapidly during the first 30 min and reached adsorption equilibrium thereafter. To investigate the adsorption mechanism, the obtained

Table 1. Adsorption isotherm constants.

Model	Parameter	Unit	MOF	Co/Fe-MOF	Ni/Fe- MOF
Langmuir	k_L	L/mg	0.02479	0.04838	0.0243
	Q_m	mg/g	658.3990	664.6904	694.2045
	R^2	–	0.99069	0.9895	0.99309
Freundlich	k_F	(mg/g)/(mg/L)$^{1/n}$	56.64048	86.85323	58.59031
	1/n	–	0.45092	0.4127	0.4539
	R^2	–	0.9748	0.94074	0.98318
Tempkin	k_T	L/mg	0.29449	0.42282	0.29784
	B_T	–	138.9804	151.0065	142.8630
	R^2	–	0.99107	0.98616	0.99308
D-R	Q_m	mg/g	469.2169	504.3617	493.2418
	E	kJ/mol	34.13592	14.02033	36.15805
	R^2	–	0.88248	0.95438	0.88054

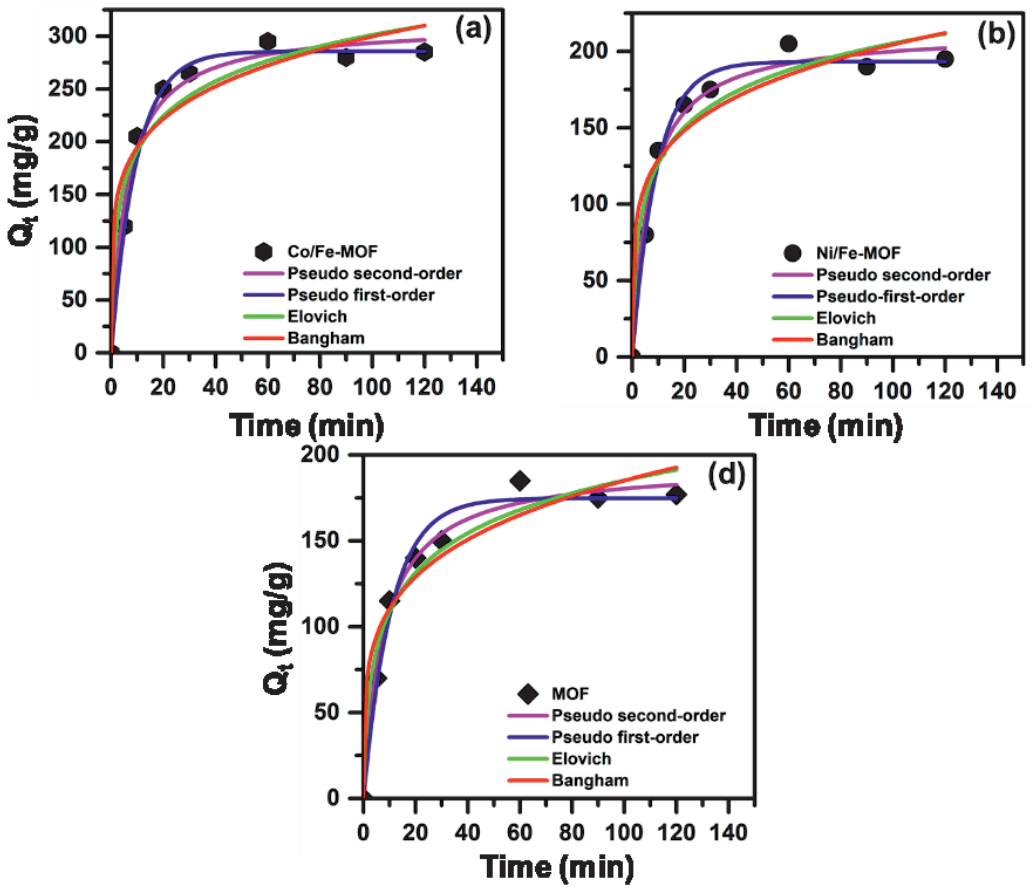

Fig. 7. The adsorption kinetic model of the materials a) Co/Fe-MOF, b) Ni/Fe-MOF, c) Fe-MOF.

kinetic data were analyzed using kinetics model. The adsorption kinetic rate constants of the materials are shown in Table 3. Dynamic data the kinetics of dye adsorption onto M/Fe-MOF (M=Ni, Co) are well agreed by the pseudo-second-order model and these results suggest that the pseudo-second-order kinetics model is satisfactory. to represent dynamic data.

Based on the calculated data in Table 2, the correlation coefficient (R^2) for all adsorption kinetic models is very high (0.91379-0.99233), showing good

Table 2. Adsorption kinetic constants.

Model	Parameter	Unit	Fe-MOF	Co/Fe-MOF	Ni/Fe- MOF
PFO	k_1	$min^{-1}/(mg/L)^{1/n}$	0.09386	0.10465	0.10755
	Q_1	mg/g	174.772	285.6268	193.287
	R^2	–	0.98	0.9646	0.98781
PSO	k_2	g/(mg.min).10^4	6.59E-4	5.31E-4	7.07E-4
	Q_2	mg/g	194.4812	311.33552	213.2443
	R^2	–	0.98763	0.98234	0.98326
Elovich	α	mg/(g.min)	81.15776	253.5016	133.5086
	β	g/mg	0.02962	0.02082	0.02905
	R^2	–	0.96083	0.93671	0.94263
Bangham	k_B	mL/(g/L)	66.0473	126.6535	81.45
	α_B	–	0.2237	0.187	0.199
	R^2	–	0.93832	0.9138	0.9202

Table 3. Comparison of CR adsorption capacity of materials from previous studies.

STT	Adsorbent material	Q_{max} (mg/g)	References
1	MIL-100(Fe) MOF	597.85	[29]
2	Sn(II)-BDC MOF	97	[24]
3	La-MOF-NH_2@Fe_3O_4	716.2	[30]
4	Fe_3O_4@Carbon	247.53	[31]
5	Fe_3O_4/MgAl-LDH	253	[32]
6	Iron oxide nanoparticle	67.1	[33]
7	MIL-68 (In)	1204	[34]
8	Cd(II)-MOF	97	[35]
9	Zn(II)-Nanoplate MOF	47	[36]
10	$Sr_5(PO4)_3(OH)/Fe_3O_4$	396	[37]
11	Fe_3O_4-cellulose nanohybrid	131	[38]
12	Fe-MOF	658	This study
13	Co/Fe-MOF	665	This study
14	Ni/Fe-MOF	694	This study

compatibility of statistical aspects of the surveyed data. However, the adsorption kinetics model is the most compatible of the four models given because R^2 is the highest. The second-order kinetics model achieved the highest correlation coefficient (0.98234-0.98595), the above results show the high compatibility and superiority of this model for the CR color adsorption process of M/Fe-MOF materials (M= Ni, Co).

In a previous publication, Dionne Dickson and co-workers also reported the high reliability of the mentioned adsorption kinetics in the adsorption process on Fe(0) iron nanoparticles from the aqueous phase, and also concluded a similarly that PSO compatibility is highest [26]. And in another study on MB and MG color adsorption of Fe_3O_4@AMCA-MIL53(Al) materials, it was also concluded that PSO is more dominant [23]. In a study on activated carbon and acid dye adsorption, the survey data also showed that this adsorption followed a second-order adsorption model [27].

Unlike the adsorption behavior described by the first-order model, where it reflects the adsorption rate relative to the number of unabsorbed sites, chemisorption usually occurs through the steps of rate control, diffusion mechanism and the influence of functional groups on the surface [28]. Here, M/Fe-MOF (M= Ni, Co) possesses a series of very active adsorption sites (basic, phenolic, lactonic and carboxylic groups) to control the chemical interaction with CR (see Table 2).

Research of Material Results

Reuse research is an important strategy in demonstrating the potential effect of "green" adsorbents on the environment. The solvent used as an effective degreasing agent is ethanol. Accordingly, Fig. 8 shows that the M/Fe-MOF (Co, Ni) materials can be reused at least four times without significant change (<16%) in adsorption capacity: from 530 mg/g (1st time) to

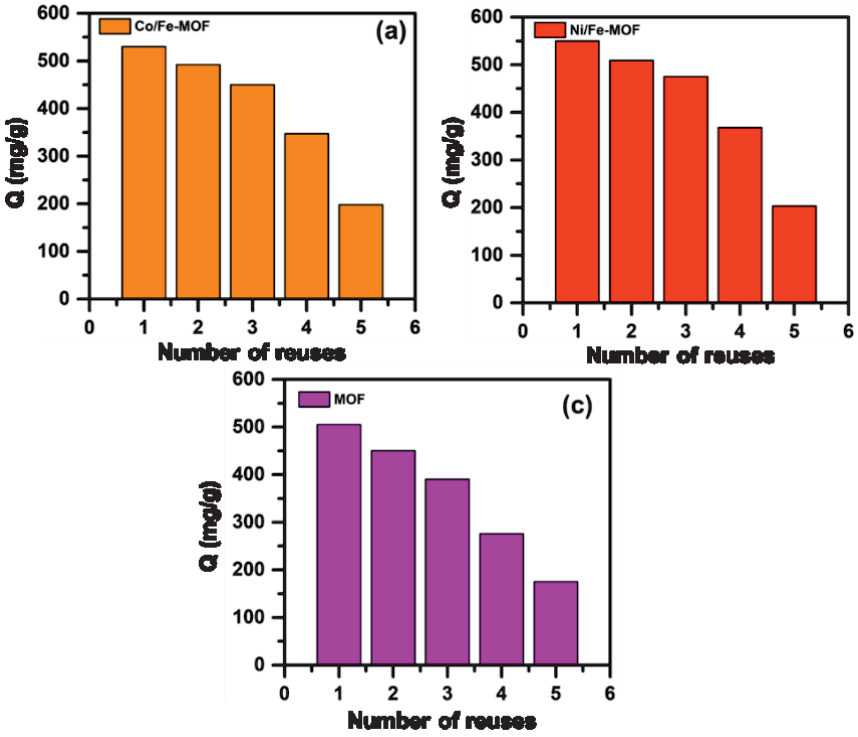

Fig. 8. Research on the reuse process.

198 mg/g (4th time) for Co/Fe-MOF materials, from 550 mg/g (1st time) to 203 mg/g (4th time) for Co/Fe-MOF materials Ni/Fe-MOF, from 505 mg/g (1st time) to 175 mg/g (4th time) for Fe-MOF materials. Thereby, demonstrating the potential to reuse M/Fe-MOF (Co, Ni, Mn) materials is very clear.

Comparing the Research Results with Other Studies

To compare the treatment efficiency of CR pigments, Table 3 summarizes the results of the maximum adsorption capacity of different materials. Compared with other studies, the maximum adsorption capacity is very high in this study, proving that the M/Fe-MOF material (M=Ni, Co) can be a promising material. for the adsorption and removal of CR colorants and for most colorants in general in aqueous medium.

Conclusions

Through the research process, survey results were obtained on the adsorption of CR pigments by M/Fe-MOF (M=Co, Ni) materials. For Co/Fe-MOF materials: The adsorption capacity reached 530 mg/g, at the colorant concentration of 75 mg/L, the adsorbent weight was 0.1 g/L and pH8. For Ni/Fe-MOF materials: The adsorption capacity is 560 mg/g, at the color concentration of 140 mg/L, the adsorbent weight is 0.1 g/L and pH8. For Fe-MOF materials: The adsorption capacity reached 523 mg/g, at the colorant concentration 120 mg/L, the adsorbent weight was 0.1 g/L and pH 8. The experimental data are consistent with Langmuir and PSO models for both M/Fe-MOF materials (M=Co, Ni). Research results on the reuse process of M/Fe-MOF (M=Co, Ni) materials show that the material is reused 4 times. With this result, it can be considered as the first step to improve the efficiency of pigment adsorption in the current water pollution treatment problem.

Acknowledgments

This research has been funded by a grant (2022.01.70/HĐ-KHCN) from the Science and Technology Development Foundation of Nguyen Tat Thanh University.

Conflict of Interests

The authors declare no conflicts of interest.

References

1. SHI Z., XU C., GUAN, H., LI L., FAN L., WANG Y., ZHANG R. Magnetic metal organic frameworks (MOFs) composite for removal of lead and malachite green in wastewater. Colloids and Surfaces A: Physicochemical and Engineering Aspects, 539, 382, **2018**.
2. PANDA J., SAHOO J.K., PANDA P.K., SAHU S.N., SAMAL M., PATTANAYAK S.K., SAHU R. Adsorptive behavior of zeolitic imidazolate framework-8 towards anionic dye in aqueous media: Combined experimental and molecular docking study. Journal of Molecular Liquids, 278, 536, **2019**.
3. AZHDARI R., MOUSAVI S.M., HASHEMI S.A., BAHRANI S., RAMAKRISHNA S. Decorated graphene with aluminum fumarate metal organic framework as a superior non-toxic agent for efficient removal of Congo Red dye from wastewater. Journal of Environmental Chemical Engineering, **7** (6), 103437, **2019**.
4. TIAN S., XU S., LIU J., HE C., XIONG Y., FENG P. Highly efficient removal of both cationic and anionic dyes from wastewater with a water-stable and eco-friendly Fe-MOF via host-guest encapsulation. Journal of Cleaner Production, 239, 117767, **2019**.
5. XUE X., WENG Y., YANG S., MENG S., ZHANG Z., YI G., ZHANG Y. Effect of Cu-based metal organic framework (Cu-MOF) loaded with TiO_2 on the photocatalytic degradation of rhodamine B dye. Environmental Science and Pollution Research, **28** (13), 15883, **2021**.
6. XIA Q., HUANG B., YUAN X., WANG H., WU Z., JIANG L., WANG H. Modified stannous sulfide nanoparticles with metal-organic framework: Toward efficient and enhanced photocatalytic reduction of chromium (VI) under visible light. Journal of Colloid and Interface Science, **530** (Vi), 481, **2018**.
7. DONG W., WANG D., WANG H., LI M., CHEN F., JIA F., YE J. Facile synthesis of In2S3/UiO-66 composite with enhanced adsorption performance and photocatalytic activity for the removal of tetracycline under visible light irradiation. Journal of Colloid and Interface Science, 535, 444, **2019**.
8. WANG H., YUAN X., WU Y., ZENG G., DONG H., CHEN X., PENG L. In situ synthesis of In2S3 at MIL-125(Ti) core-shell microparticle for the removal of tetracycline from wastewater by integrated adsorption and visible-light-driven photocatalysis. Applied Catalysis B: Environmental, 186, 19, **2016**.
9. DADFARNIA S., HAJI SHABANI A.M., MORADI S.E., EMAMI S. Methyl red removal from water by iron based metal-organic frameworks loaded onto iron oxide nanoparticle adsorbent. Applied Surface Science, **330** (2015), 85, **2015**.
10. DZHARDIMALIEVA G.I., BAIMURATOVA R.K., KNERELMAN E I., DAVYDOVA, G.I., KUDAIBERGENOV S.E., &KHARISSOVA O.V. Synthesis of Copper (II) Trimesinate Coordination Polymer and Its Use as a Sorbent for Organic Dyes and a Precursor for Nanostructured Material, (**Ii**). **(n.d.)**
11. DELPIANO G.R., TOCCO D., MEDDA L., MAGNER E. Adsorption of Malachite Green and Alizarin Red S Dyes Using Fe-BTC Metal Organic Framework as Adsorbent. **2021**.
12. BDC C., CATIONIC A., DYES A., KIM T., TRAN,N., PHUONG C., NGUYEN O. Synthesis and Characterization Bimetallic Organic Framework CoxFex (BDC) and Adsorption Cationic and Anionic Dyes, 1. **2022**.
13. XUE Z., WANG Y., ZHANG Y., FAN G., HAN S., PAN J. Construction of Cu(I)-Organic Frameworks with Effective Sorption Behavior for Iodine and Congo Red, (**I**). **2022**.

14. BACH L.G., VAN TRAN T., NGUYEN T.D., VAN PHAM T., DO S.T. Enhanced adsorption of methylene blue onto graphene oxide-doped XFe2O4 (X = Co, Mn, Ni) nanocomposites: kinetic, isothermal, thermodynamic and recyclability studies. Research on Chemical Intermediates, **44** (3), 1661, **2018**.
15. PURKAIT M.K., MAITI A., DASGUPTA S., DE S. Removal of congo red using activated carbon and its regeneration. Journal of Hazardous Materials, **145** (1-2), 287, **2007**.
16. LEI C., ZHU X., ZHU B., YU J., HO W. Hierarchical NiO–SiO_2 composite hollow microspheres with enhanced adsorption affinity towards Congo red in water. Journal of Colloid and Interface Science, 466, 238, **2016**.
17. BAO Y., QIN M., YU Y., ZHANG L., WU H. Facile fabrication of porous $NiCo_2O_4$ nanosheets with high adsorption performance toward Congo red. Journal of Physics and Chemistry of Solids, 124, 289, **2019**.
18. ZHANG G., WO R., SUN Z., HAO G., LIU G., ZHANG Y., JIANG W. Effective Magnetic MOFs Adsorbent for the Removal of Bisphenol A, Tetracycline, Congo Red and Methylene Blue Pollutions. Nanomaterials, **11** (8), 1917, **2021**.
19. NI W., XIAO X., GENG W., ZHANG L., LI Y., LI N. Controllable preparation of amino-functionalized ZIF-8: A functionalized MOF material for adsorbing Congo Red and Eriochrome Black T in aqueous solution. JCIS Open, 3, 100018, **2021**.
20. FU Q., LOU J., ZHANG R., PENG L., ZHOU S., YAN W., LUO J. Highly effective and fast removal of Congo red from wastewater with metal-organic framework Fe-MIL-88NH2. Journal of Solid State Chemistry, 294, 121836, **2021**.
21. LIAN L., GUO L., GUO C. Adsorption of Congo red from aqueous solutions onto Ca-bentonite. Journal of Hazardous Materials, **161** (1), 126, **2009**.
22. MIRSOLEIMANI-AZIZI S.M., SETOODEH P., ZEINALI S., RAHIMPOUR M.R. Tetracycline antibiotic removal from aqueous solutions by MOF-5: Adsorption isotherm, kinetic and thermodynamic studies. Journal of Environmental Chemical Engineering, **6** (5), 6118, **2018**.
23. ALQADAMI A.A., NAUSHAD M., ALOTHMAN Z.A., AHAMAD T. Adsorptive performance of MOF nanocomposite for methylene blue and malachite green dyes: Kinetics, isotherm and mechanism. Journal of Environmental Management, 223, 29, **2018**.
24. GHOSH A., DAS G. Green synthesis of Sn(II)-BDC MOF: Preferential and efficient adsorption of anionic dyes. Microporous and Mesoporous Materials, 297, 110039, **2020**.
25. VALADI F.M., EKRAMIPOOYA A., GHOLAMI M.R., Selective separation of Congo Red from a mixture of anionic and cationic dyes using magnetic-MOF: Experimental and DFT study, J. Mol. Liq. **318**, 114051, **2020** Doi: 10.1016/j.molliq.2020.114051
26. DICKSON D., LIU G., CAI Y. Adsorption kinetics and isotherms of arsenite and arsenate on hematite nanoparticles and aggregates. Journal of Environmental Management, 186, 261, **2017**.
27. GÓMEZ V., LARRECHI M.S., CALLAO M.P. Kinetic and adsorption study of acid dye removal using activated carbon. Chemosphere, **69** (7), 1151, **2007**.
28. INYINBOR A.A., ADEKOLA F.A., OLATUNJI G.A. Kinetics, isotherms and thermodynamic modeling of liquid phase adsorption of Rhodamine B dye onto Raphia hookerie fruit epicarp. Water Resources and Industry, 15, 14, **2016**.
29. MORADI S.E., DADFARNIA S., HAJI SHABANI A.M., EMAMI S. Removal of congo red from aqueous solution by its sorption onto the metal organic framework MIL-100(Fe): equilibrium, kinetic and thermodynamic studies. Desalination and Water Treatment, **56** (3), 709, **2015**.
30. VALADI F.M., EKRAMIPOOYA A., GHOLAMI M.R. Selective separation of Congo Red from a mixture of anionic and cationic dyes using magnetic-MOF: Experimental and DFT study. Journal of Molecular Liquids, 318, 114051. **2020**
31. REN L., LIN H., MENG F., ZHANG F. One-step solvothermal synthesis of Fe_3O_4@Carbon composites and their application in removing of Cr (VI) and Congo red. Ceramics International, **45** (7), 9646, **2019**.
32. SHAN R., YAN L., YANG K., YU S., HAO Y., YU H., DU B. Magnetic Fe_3O_4/MgAl-LDH composite for effective removal of three red dyes from aqueous solution. Chemical Engineering Journal, 252, 38, **2014**.
33. SAHA B., DAS S., SAIKIA J., DAS G. Preferential and Enhanced Adsorption of Different Dyes on Iron Oxide Nanoparticles: A Comparative Study. The Journal of Physical Chemistry C, **115** (16), 8024, **2011**.
34. JIN L.-N., QIAN X.-Y., WANG J.-G., ASLAN H., DONG M. MIL-68 (In) nano-rods for the removal of Congo red dye from aqueous solution. Journal of Colloid and Interface Science, 453, 270, **2015**.
35. MASOOMI M.Y., BAGHERI M., MORSALI A. Porosity and dye adsorption enhancement by ultrasonic synthesized Cd(II) based metal-organic framework. Ultrasonics Sonochemistry, 37, 244, **2017**.
36. ABDOLLAHI N., MASOOMI M.Y., MORSALI A., JUNK P.C., WANG J. Sonochemical synthesis and structural characterization of a new Zn(II) nanoplate metal-organic framework with removal efficiency of Sudan red and Congo red. Ultrasonics Sonochemistry, 45, 50, **2018**.
37. ZHANG F., YIN X., ZHANG W. Development of magnetic Sr 5 (PO_4) 3(OH)/Fe_3O_4 nanorod for adsorption of Congo red from solution. Journal of Alloys and Compounds, 657, 809, **2016**.
38. BEYKI M.H., BAYAT M., SHEMIRANI F. Fabrication of core-shell structured magnetic nanocellulose base polymeric ionic liquid for effective biosorption of Congo red dye. Bioresource Technology, 218, 326, **2016**.